Published by Avanti Publishers

Global Journal of Energy Technology Research Updates

ISSN (online): 2409-5818

Visualization Experiments of Radial-Rotating Oscillating Heat Pipe Filled with Methanol

Jiaren Wang[1], Ning Qian[1,2,*] and Yucan Fu[1,2]

[1]*College of Mechanical and Electrical Engineering, Nanjing University of Aeronautics and Astronautics, Nanjing 210016, China*

[2]*Jiangsu Key Laboratory of Precision and Micro-Manufacturing Technology, Nanjing University of Aeronautics and Astronautics, Nanjing 210016, China*

ARTICLE INFO

Article Type: Research Article

Keywords:
Flow pattern
Visualization
Motion mode
Radial-rotating oscillating heat pipe

Timeline:
Received: October 25, 2023
Accepted: November 28, 2023
Published: December 09, 2023

Citation: Wang J, Qian N, Fu Y. Visualization experiments of radial-rotating oscillating heat pipe filled with methanol. Glob J Energ Technol Res Updat. 2023; 10: 24-32.

DOI: https://doi.org/10.15377/2409-5818.2023.10.2

ABSTRACT

Oscillating heat pipes (OHP) have highly efficient heat transfer capability. Some researchers have applied OHPs to cutting tools and rotating machines by embedding tubular OHPs in machines or by making flow channels on metal plates. Most studies are on heat transfer performance, and there are few studies on the heat transfer behavior of radial-rotating oscillating heat pipes (RR-OHP) under operating conditions. This paper conducted the visualization test of an RR-OHP filled with methanol by studying the flow patterns and motion modes at rotation speed (0-860 rpm) and heat flux (20000-40000 W/m^2). When the heat flux is increased from 20000 W/m^2 to 40000 W/m^2, the flow patterns include flowless, slug flow, annular flow, and churn flow, and the motion modes contain oscillatory motion, cyclic motion, unilateral boiling, and bilateral boiling. The distribution map of the flow patterns and motion modes with the centrifugal acceleration and the heat flux was plotted, which shows the evolution of the flow patterns and the transformation of the motion modes of the RR-OHP, and elucidates the effect of the centrifugal acceleration and the heat flux on the flow patterns and motion modes.

*Corresponding Author
Email: n.qian@nuaa.edu.cn
Tel: +(86) 258 489 0644

1. Introduction

In the 1990s, oscillating heat pipes were developed, constructed from capillary tubes with three sections: evaporator, condenser, and adiabatic section. Its heat transfer modes include phase-change heat transfer, vapor-liquid plug movement to transfer sensible heat, and expansion work [1-4]. Its simple structure, high heat transfer efficiency, passive heat transfer, and good adaptability make it an ideal heat transfer element [5-7]. Due to its good heat transfer capability, researchers have applied OHPs to cutting tools and rotating machines by embedding tubular OHPs in machines or by making flow channels on metal plates to form flat plate OHPs [8-12].

There are many studies on oscillating heat pipes in static conditions, mainly from heat transfer performance [13-20], visualization [21-27], and numerical simulation studies [28-34]. However, relatively few studies exist on rotating oscillating heat pipes compared to OHP. The rotating oscillating heat pipes are divided into axial-rotating oscillating heat pipes (AR-OHPs) and radial-rotating oscillating heat pipes (RR-OHPs). Relevant studies show that increasing centrifugal acceleration and heat flux will improve the heat transfer performance of the AR-OHP. Its speed is increased and its circulation process is accelerated, and the change of flow patterns is also analyzed [35]. It starts up well when centrifugal acceleration varies between 0 and 738 m/s^2. In the critical diameter range, the larger the inner diameter, the shorter the start-up time, and the earlier the AR-OHP starts to use its heat transfer capacity, therefore, the diameter of the AR-OHP was selected as 3 mm, and acetone was used as the working fluid [36, 37]. In a heat transfer test where the flux varied from 73.8 to 98.4 kW/m^2 and the rotation speed varied from 0 to 300 rpm, the flower-shaped AR-OHP resulted in an improvement in heat transfer. [38, 39]. During dry grinding, the AR-OHP grinding wheel can successfully reduce high temperatures when grinding difficult-to-grind materials, reduce grinding wheel wear, and extend grinding wheel life [40, 41].

Studies with RR-OHPs have shown that they have good heat transfer performance at 800 rpm and a 50% filling rate [42]. Heat pipes oscillating under centrifugal acceleration exhibit a positive thermal conductivity [43]. It is possible to reduce the thermal resistance by increasing centrifugal acceleration and heat flux, but this should not be done at the expense of increasing it too much [44]. As the RR-OHP reaches a critical state, its heat transfer performance will deteriorate [45]. Heat transfer performance of rar-OHPs is correlated with the dimensionless number, according to Liu *et al*. [46]. The non-uniform arrangement helps the RR-OHP to circulate unidirectionally, so the heat transfer performance is good [47]. Chen *et al*. investigated the change in the flow pattern of RR-OHP and AR-OHP at a =40 m/s^2 [48, 49], but the visualization study with higher centrifugal acceleration was not addressed. A related study confirmed the effectiveness of radial rotation at high centrifugal accelerations [50], demonstrating the feasibility of RR-OHP wheels. However, the phenomenon of the appearance of the transition point in its heat transfer performance and how the centrifugal acceleration affects the motion of the RR-OHP is not clarified, so it is necessary to conduct the visualization test of the RR-OHP at a high rotation speed to illustrates its heat transfer behavior and provide theoretical support for the design of the RR-OHP machine.

The visualization test of the RR-OHP will be carried out under simulated grinding conditions. It will reveal the evolution of flow patterns and the change of motion modes by observing the motion process of the internal working fluid, and the role of centrifugal acceleration on the RR-OHP will be elucidated as well as heat flux.

2. Experimental Setup and Description

The visualization test of the RR-OHP (in the rotating state of the OHP arranged radially along the rotating axis) is carried out relying on the visualization test device (Fig. **1**). In the test, the inner diameter of a glass single-loop OHP is 3 mm, and it is filled with methanol at a 50% filling rate. It is installed on the rotating support whose length is 400 mm and installed on a lathe to adjust the rotation speed. The centrifugal acceleration at different rotation speeds can be calculated according to Eq. 1. The EVA housing is used to ensure that the glass OHP does not break under rotational conditions. The brush-slip ring is used to connect the nickel-chromium resistance wire with the QJ3003SⅢ DC voltage regulator to achieve the heating of the evaporator under rotating conditions, and the vortex tube is used for cooling. The experimental parameters are shown in Table **1**.

$$a = \omega^2 r = (\frac{n\pi}{30})^2 r \quad (1)$$

where a is the centrifugal acceleration (unit: m/s^2), n is the rotational speed (unit: rpm), ω is the angular velocity (unit: rad/s), and r is the rotational radius (unit: m).

Table 1: Parameters of visualization test.

Test Condition	Test Parameters
Ambient temperature	20 °C
Working fluid	Methanol
Filling rate	50%
Heat flux (W/m2)	20000, 25000, 30000, 35000, 40000
Rotation speed (rpm)	0, 140, 280, 430, 580, 716, 860
Centrifugal acceleration (m/s2)	0, 43, 172, 406, 737, 1124, 1622
Cooling method	0.4 MPa cold air cooling

A ring light source is used to ensure uniformity of light during shooting. By adjusting the distance and angle difference between the shooting support and the rotating support, and using axial and circumferential fixation to prevent axial movement and circumferential rotation, the filming equipment can focus on the RR-OHP all the time without shaking. To obtain an image of the oscillating heat pipe in rotation, we need to turn the machine on and apply the centrifugal force after it has run smoothly in a stationary state. So the rotating support is first adjusted to the vertical position, the cooling is switched on and the bottom is heated vertically in the static state. When the OHP has been working stably for 30-60 seconds, the machine tool is started up, and then the wireless remote control is used to open the high frame rate filming equipment and start filming. To ensure that the image can identify the flow patterns and motion modes, the high frame rate filming equipment shoots for 2 minutes at 240 fps and then shoots for 10 seconds at 960 fps for several segments. At the end of the test, the heating system is switched off and cooling is continued until the OHP has cooled sufficiently to ambient temperature to ensure that each test is independent of the other. Each test must be repeated 3 times to ensure the accuracy of the data.

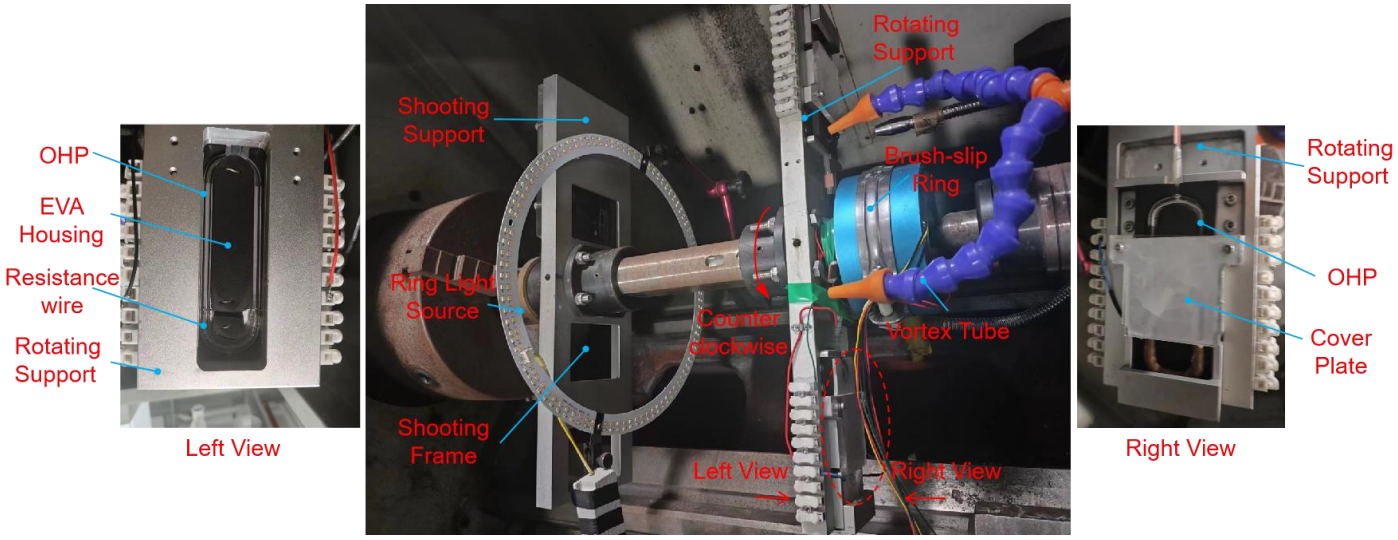

Figure 1: Visualization test device.

3. Results and Discussion

3.1. The Evolution of the Flow Patterns

The flow patterns of the RR-OHP (a = 0 m/s^2) include slug flow and annular flow. Slug flow (Fig. **2b**) occurs when its diameter is close to the internal flow channel of the RR-OHP, the bubble morphology is complete and belongs to the Taylor bubble. The tracked bubbles move from the evaporator to the condenser, where they grow and develop in the adiabatic section and condense into the liquid phase when they reach the condenser. the bubble length of the slug flow continues to increase and a long slug plug is formed until the annular flow appears (Fig. **2c**) with the increasing heat flux, which occurs when the bubble in the evaporator is heated to become a long slug plug through the adiabatic section, which generates an annular liquid film, with the traced slug plug passing through the condenser and returning, the annular liquid film gradually moves towards the condenser, and finally disappears at the condenser, and the following long slug plug moves to the evaporator end near the inlet of the other side of the RR-OHP, and the new slug plug is about to develop into an annular flow. At low heat flux, annular flow cannot be generated due to insufficient driving force.

RR-OHP (a > 0 m/s^2) has four kinds of flow patterns. Two of them are the same as the RR-OHP (a = 0 m/s^2), the others are its unique flow patterns. The flowless (Fig. **2a**) occurs with no phase generating. The churn flow (Fig. **2d**) occurs as the deformation of bubbles, and due to the violent movement of the liquid flow, which leads to the breakage of the bubbles, the formation of various sizes of air mass, and the bubbles move chaotically towards the condenser in the liquid flow. Churn flow is related to the centrifugal acceleration and only occurs when the centrifugal acceleration reaches a certain value.

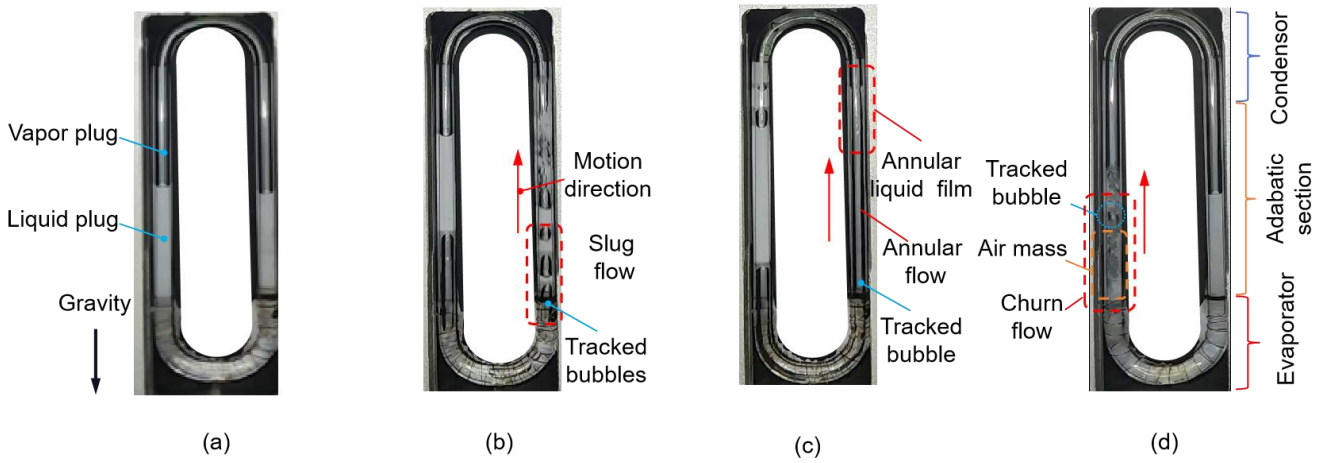

Figure 2: Flow pattern: (**a**) Flowless, (**b**) Slug flow, (**c**) Annular flow, and (**d**) Churn flow.

As shown in Fig. (**3**), when the RR-OHP runs smoothly, its flow pattern is mainly slug flow. With increasing heat flux, the flow pattern of RR-OHP changes from slug flow to annular flow at rotation speeds n = 0 rpm and n = 140 rpm, and the length of the bubbles increases. Due to the smaller centrifugal acceleration at this speed, which has little effect on the RR-OHP, the flow pattern under rotational conditions is similar to stationary. When n = 280 rpm and n = 430 rpm, the flow pattern of RR-OHP is slug flow and the length of the vapor plug is increasing, annular flow is not observed at this time because the increase in centrifugal acceleration limits it and this condition makes it hard for annular flow to occur. When n = 580 rpm, n = 716 rpm, and n = 860 rpm, the flow pattern of RR-OHP changes from flowless to slug flow and then into churn flow. This is because the boiling point increases with high centrifugal force, resulting in the RR-OHP at low heat flux where there is no phase change generated. At high heat flux, the RR-OHP begins to appear slug flow due to the temperature of the evaporator increases, and even the emergence of churn flow of this new flow type, which is due to the high centrifugal force and the high driving force of the combined effect of the surface morphology of the bubbles is destroyed, the formation of violent movement of the air mass and the phenomenon of the broken small bubbles in the tube movement.

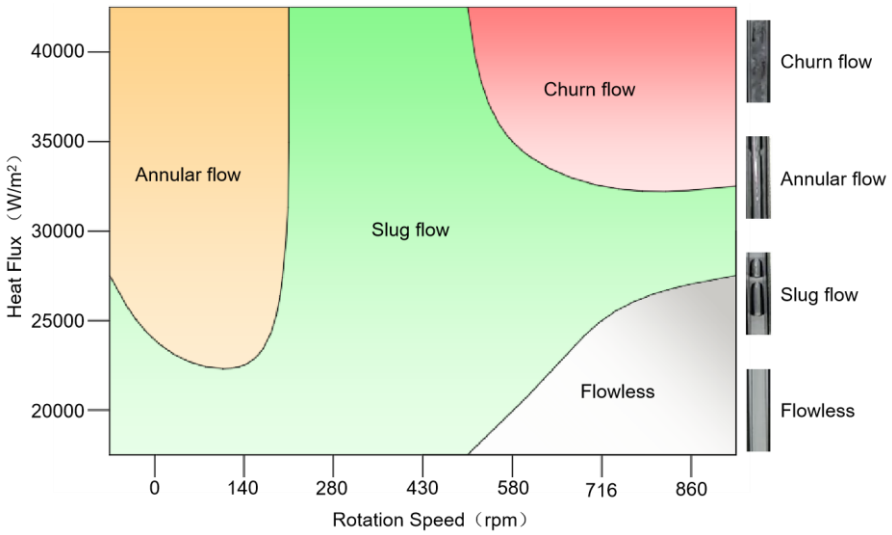

Figure 3: Flow pattern distribution map.

In conclusion, in test conditions, the main flow pattern is slug flow. The flow pattern evolves into churn flow with centrifugal acceleration and heat flux, and there is a transitional phase in which the two types of flow patterns appear alternately. The centrifugal acceleration determines the final flow pattern of the RR-OHP, while the heat flux influences the evolution of the flow pattern by affecting the intensity of motion and the length of the vapor plug.

3.2. The Transformations of the Motion Modes

The motion modes of RR-OHP (a = 0 m/s^2) include oscillatory motion and cyclic motion. As shown in Fig. (**4a**), the tracked bubble moves counterclockwise with time, grows to form a long slug plug at the adiabatic section, then passes through the condenser bend and begins to condense, it becomes small, refluxes along the adiabatic section and then returns to the evaporator and grows again at the evaporator to complete the cyclic process. The tracked bubble moves first clockwise and then counterclockwise with time in Fig. (**4b**). It moves to the condenser and condenses, without going through the condenser bend, because of the pressure along the adiabatic section and back to the evaporator, and then through the evaporator bend, the bubble grows, its length increases, and then arrives at the condenser and returns to the evaporator, such a reciprocating motion is an oscillatory motion.

The motion modes of the RR-OHP (a > 0 m/s^2) include cyclic motion, oscillatory motion, unilateral boiling, and bilateral boiling. Their cyclic motion and oscillatory motion are similar to the motion modes of RR-OHP (a = 0 m/s^2), so they are not repeated here. As shown in Fig. (**4c**), it is the unilateral boiling, where the tracked bubble moves clockwise with time, moving from the outlet of the evaporator, growing and increasing its volume, to the inlet of the condenser, condensing into the liquid phase and forming a liquid film. With the effect of the centrifugal force, it returns to the evaporator along the same side of the adiabatic section, and the other side of the RR-OHP does not generate bubbles. As shown in Fig. (**4d**), the bilateral boiling is pretty similar to the unilateral boiling, we can see that the bilateral boiling is the upgrade motion mode. The bilateral boiling process of the slug plug with the development of time, and the process of the tracked bubble is similar to the unilateral boiling. The bubble of bilateral boiling goes from both sides of the evaporator to the condenser. Near the condenser inlet, it condenses to the liquid phase, refluxes on the same side, and returns to the evaporator with the effect of the centrifugal force.

As shown in Fig. (**5**), when the RR-OHP runs smoothly, its main motion modes are unilateral boiling and bilateral boiling. With increasing heat flux, when the rotation speed n =0 rpm and n =140 rpm, the motion mode is transformed from oscillatory motion to cyclic motion, which is due to the insufficient driving force at the low heat flux, and the working fluid does not pass through the condenser bends by the effect of the motion resistance and the driving force is large at the high heat flux so that it can realize the cyclic motion. Due to the small centrifugal

force, the motion form of the RR-OHP is the same as that in the stationary state. When *n* =280, 430, 580, 716, and 860 rpm, the RR-OHP appeared to be unilateral boiling and bilateral boiling two new forms of motion. Its motion mode changes from oscillatory motion to unilateral boiling and then to bilateral boiling, due to the increase in centrifugal acceleration, the working fluid of the movement of the resistance increases, making it difficult to pass through the bend at the end of the condenser but directly condensing back to the evaporator with the capillary phenomenon weakened, so there is a unilateral boiling. With increasing heat flux, the movement of the RR-OHP intensifies the emergence of bilateral boiling with the driving force increasing. The movement process of these two processes is shortened, so the circulation is accelerated.

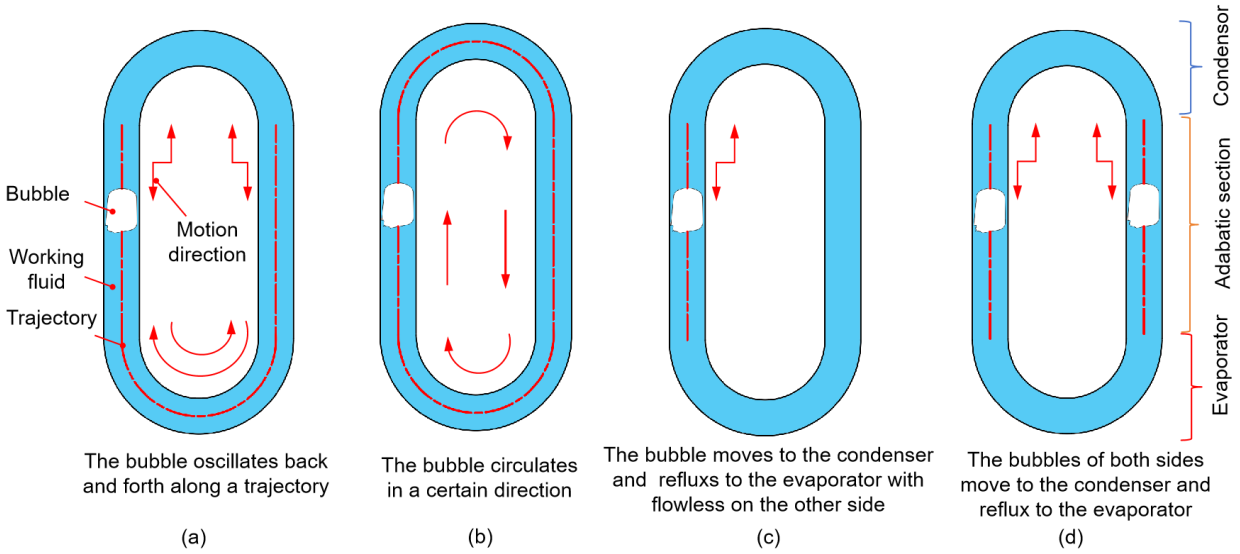

Figure 4: Motion mode: (**a**) Oscillatory motion, (**b**) Cyclic motion, (**c**) Unilateral boiling, and (**d**) Bilateral boiling.

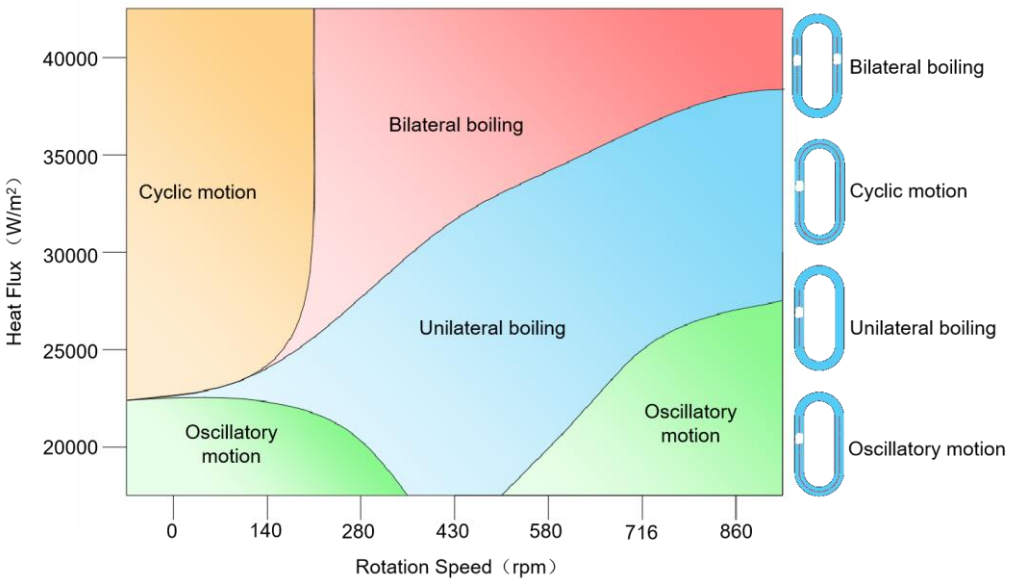

Figure 5: Motion mode distribution map.

In conclusion, in the test conditions, the main motion modes are unilateral boiling and bilateral boiling. As the centrifugal acceleration and heat flux increase, the motion mode changes to bilateral boiling, and the transition process is smooth and non-abrupt. The motion mode of the RR-OHP is closely related to the centrifugal acceleration and heat flux. At low centrifugal acceleration, the motion mode changes from oscillatory motion to cyclic motion. At high centrifugal acceleration, the oscillatory motion changes to unilateral boiling and then to bilateral boiling.

4. Conclusion

This paper studies the flow patterns and motion modes of RR-OHP with different centrifugal accelerations and heat fluxes. It reveals the evolution of the flow pattern and the transformations of the motion mode and elucidates the principle of centrifugal acceleration and heat flux on the flow pattern and motion mode, and the flowing is the conclusions:

When the heat flux is increased from 20000 W/m^2 to 40000 W/m^2, the flow pattern of RR-OHP will gradually change to churn flow and its motion mode will change to bilateral boiling. Flow pattern evolution and motion mode transformation are smooth and non-abrupt. The main flow pattern of RR-OHP filled with methanol is slug flow and the main motion modes of it are unilateral boiling and bilateral boiling.

The flow pattern is strongly correlated with the centrifugal acceleration. When the heat flux is increased from 20000 W/m^2 to 40000 W/m^2, the flow pattern changes from flowless to slug flow and then into annular flow or churn flow. The centrifugal acceleration determines the final flow pattern of the evolution of the flow patterns. The final flow pattern is annular flow when a < 172 m/s^2 and it is churn flow when a > 172 m/s^2. The heat flux affects the evolution process by influencing the intensity of the movement and the timeshare of different flow patterns.

The motion mode is closely related to the heat flux and centrifugal acceleration. When the heat flux increases from 20000 W/m^2 to 40000 W/m^2, the motion mode changes from oscillatory motion to cyclic motion when a < 172 m/s^2, from unilateral boiling to bilateral boiling when 172 m/s^2< a < 737 m/s^2 and it is transformed from oscillatory motion to unilateral boiling and then into bilateral boiling when a > 737 m/s^2.

Nomenclature

RR-OHP = Radial-rotating oscillating heat pipes

AR-OHP = Axial-rotating oscillating heat pipes

OHP = Oscillating heat pipes

Conflict of Interests

The authors declare no competing interests.

Funding

This work was financially supported by the National Natural Science Foundation of China (Grant No. 52205476), Youth Talent Support Project of Jiangsu Provincial Association of Science and Technology (Grant No. TJ-2023-070), Science Center for Gas Turbine Project (No. P2022-AB-IV-002-001), and the Fund of Prospective Layout of Scientific Research for NUAA (Grant No. 1005-LA22001).

Acknowledgment

I wish to acknowledge Dr. Jiang, Philosophic Doctor of Nanjing University of Aeronautics and Astronautics, for her precious advice on experimental design. I wish to thank the Institution of High Efficiency Precision Machining Technology, for the help in conducting the experiment.

References

[1] Sathe TM, Wankhede US. Review on closed loop oscillating heat pipe. Int J Eng Res Technol. 2014; 3: 1195-201.

[2] Han X, Wang X, Zheng H, Xu X, Chen G. Review of the development of pulsating heat pipe for heat dissipation. Renew Sustain Energy Rev. 2016; 59: 692-709. https://doi.org/10.1016/j.rser.2015.12.350

[3] Ma HB, Borgmeyer B, Cheng P, Zhang Y. Heat transport capability in an oscillating heat pipe. J Heat Transfer. 2008; 130(8): 081501. https://doi.org/10.1115/1.2909081

[4] Ma H. Oscillating heat pipes. New York, NY: Springer New York; 2015. https://doi.org/10.1007/978-1-4939-2504-9

[5] Liu X, Han X, Wang Z, Hao G, Zhang Z, Chen Y. Application of an anti-gravity oscillating heat pipe on enhancement of waste heat recovery. Energy Convers Manag. 2020; 205: 112404. https://doi.org/10.1016/j.enconman.2019.112404

[6] Qu J, Guan F, Lv Y, Wang Y. Experimental study on the heat transport capability of micro-grooved oscillating heat pipe. Case Stud Therm Eng. 2021; 26: 101210. https://doi.org/10.1016/j.csite.2021.101210

[7] Im YH, Lee JY, Ahn TI, Youn YJ. Operational characteristics of oscillating heat pipe charged with R-134a for heat recovery at low temperature. Int J Heat Mass Transf. 2022; 196: 123231. https://doi.org/10.1016/j.ijheatmasstransfer.2022.123231

[8] Liu X, Chen X, Zhang Z, Chen Y. Thermal performance of a novel dual-serpentine-channel flat-plate oscillating heat pipe used for multiple heat sources and sinks. Int J Heat Mass Transf. 2020; 161: 120293. https://doi.org/10.1016/j.ijheatmasstransfer.2020.120293

[9] Lin Z, Wang S, Huo J, Hu Y, Chen J, Zhang W, *et al*. Heat transfer characteristics and LED heat sink application of aluminum plate oscillating heat pipes. Appl Therm Eng. 2011; 31: 2221-9. https://doi.org/10.1016/j.applthermaleng.2011.03.003

[10] Wu Z, Xing Y, Liu L, Huang P, Zhao G. Design, fabrication and performance evaluation of pulsating heat pipe assisted tool holder. J Manuf Process. 2020; 50: 224-33. https://doi.org/10.1016/j.jmapro.2019.12.054

[11] Wu Z, Deng J, Su C, Luo C, Xia D. Performance of the micro-texture self-lubricating and pulsating heat pipe self-cooling tools in dry cutting process. Int J Refract Metals Hard Mater. 2014; 45: 238-48. https://doi.org/10.1016/j.ijrmhm.2014.02.004

[12] Wu Z, Bao H, Xing Y, Liu L. Dry cutting performance and heat transfer simulation of pulsating heat pipe self-cooling tool holder. J Manuf Process. 2022; 83: 129-42. https://doi.org/10.1016/j.jmapro.2022.08.055

[13] Ji Y, Ma H, Su F, Wang G. Particle size effect on heat transfer performance in an oscillating heat pipe. Exp Therm Fluid. 2011; 35: 724-7. https://doi.org/10.1016/j.expthermflusci.2011.01.007

[14] Ma HB, Wilson C, Yu Q, Park K, Choi US, Tirumala M. An experimental investigation of heat transport capability in a nanofluid oscillating heat pipe. J Heat Transfer. 2006; 128: 1213-6. https://doi.org/10.1115/1.2352789

[15] Hao T, Ma X, Lan Z, Li N, Zhao Y, Ma H. Effects of hydrophilic surface on heat transfer performance and oscillating motion for an oscillating heat pipe. Int J Heat Mass Transf. 2014; 72: 50–65. https://doi.org/10.1016/j.ijheatmasstransfer.2014.01.007

[16] Jung C, Kim SJ. Effects of oscillation amplitudes on heat transfer mechanisms of pulsating heat pipes. Int J Heat Mass Transf. 2021; 165: 120642. https://doi.org/10.1016/j.ijheatmasstransfer.2020.120642

[17] Jo J, Kim J, Kim SJ. Experimental investigations of heat transfer mechanisms of a pulsating heat pipe. Energy Convers Manag. 2019; 181: 331–41. https://doi.org/10.1016/j.enconman.2018.12.027

[18] Liu X, Chen Y. Fluid flow and heat transfer in flat-plate oscillating heat pipe. Energy Build. 2014; 75: 29-42. https://doi.org/10.1016/j.enbuild.2014.01.041

[19] Nuntaphan A, Vithayasai S, Vorayos N, Vorayos N, Kiatsiriroat T. Use of oscillating heat pipe technique as extended surface in wire-on-tube heat exchanger for heat transfer enhancement. Int Commun Heat Mass Transfer. 2010; 37: 287–92. https://doi.org/10.1016/j.icheatmasstransfer.2009.11.006

[20] Iwata N, Miyazaki Y, Yasuda S, Ogawa H. Thermal performance and flexibility evaluation of metallic micro oscillating heat pipe for thermal strap. Appl Therm Eng. 2021; 197: 117342. https://doi.org/10.1016/j.applthermaleng.2021.117342

[21] Li Q-M, Zou J, Yang Z, Duan Y-Y, Wang B-X. Visualization of two-phase flows in nanofluid oscillating heat pipes. J Heat Transfer. 2011; 133: 11–5. https://doi.org/10.1115/1.4003043

[22] Xu JL, Li YX, Wong TN. High speed flow visualization of a closed loop pulsating heat pipe. Int J Heat Mass Transf. 2005; 48: 3338-51. https://doi.org/10.1016/j.ijheatmasstransfer.2005.02.034

[23] Su Z, Hu Y, Zheng S, Wu T, Liu K, Zhu M, *et al*. Recent advances in visualization of pulsating heat pipes: A review. Appl Therm Eng. 2023; 221: 119867. https://doi.org/10.1016/j.applthermaleng.2022.119867

[24] Spinato G, Borhani N, d'Entremont BP, Thome JR. Time-strip visualization and thermo-hydrodynamics in a closed loop pulsating heat pipe. Appl Therm Eng. 2015; 78: 364-72. https://doi.org/10.1016/j.applthermaleng.2014.12.045

[25] Yasuda Y, Nabeshima F, Horiuchi K, Nagai H. Visualization of the working fluid in a flat-plate pulsating heat pipe by neutron radiography. J Heat Mass Transf. 2022; 185: 122336. https://doi.org/10.1016/j.ijheatmasstransfer.2021.122336

[26] Zhang D, He Z, Guan J, Tang S, Shen C. Heat transfer and flow visualization of pulsating heat pipe with silica nanofluid: An experimental study. Int J Heat Mass Transf. 2022; 183: 122100. https://doi.org/10.1016/j.ijheatmasstransfer.2021.122100

[27] Senjaya R, Inoue T. Bubble generation in oscillating heat pipe. Appl Therm Eng. 2013; 60: 251-5. https://doi.org/10.1016/j.applthermaleng.2013.06.041

[28] Schwarz F, Uddehal SR, Lodermeyer A, Bagheri EM, Forster-Heinlein B, Becker S. Interaction of flow pattern and heat transfer in oscillating heat pipes for hot spot applications. Appl Therm Eng. 2021; 196: 117334. https://doi.org/10.1016/j.applthermaleng.2021.117334

[29] Adachi T, Chang X, Nagai H, Takahashi S. Numerical investigation on necessary condition for temperature oscillation in loop heat pipe. Int J Therm Sci. 2024; 196: 108704. https://doi.org/10.1016/j.ijthermalsci.2023.108704

[30] Maghrabie HM, Olabi AG, Alami AH, Radi M Al, Zwayyed F, Salamah T, *et al*. Numerical simulation of heat pipes in different applications. Int J Thermofluids. 2022; 16: 100199. https://doi.org/10.1016/j.ijft.2022.100199

[31] Daimaru T, Nagai H, Ando M, Tanaka K, Okamoto A, Sugita H. Comparison between numerical simulation and on-orbit experiment of oscillating heat pipes. Int J Heat Mass Transf. 2017; 109: 791-806. https://doi.org/10.1016/j.ijheatmasstransfer.2017.01.078

[32] Zhao J, Wu C, Rao Z. Numerical study on heat transfer enhancement of closed loop oscillating heat pipe through active incentive method. Int Commun Heat Mass Transfer. 2020; 115: 104612. https://doi.org/10.1016/j.icheatmasstransfer.2020.104612

[33] Vo D-T, Kim H-T, Ko J, Bang K-H. An experiment and three-dimensional numerical simulation of pulsating heat pipes. Int J Heat Mass Transf. 2020; 150: 119317. https://doi.org/10.1016/j.ijheatmasstransfer.2020.119317

[34] Daimaru T, Yoshida S, Nagai H. Study on thermal cycle in oscillating heat pipes by numerical analysis. Appl Therm Eng. 2017; 113: 1219-27. https://doi.org/10.1016/j.applthermaleng.2016.11.114

[35] On-ai K, Kammuang-lue N, Terdtoon P, Sakulchangsatjatai P. Implied physical phenomena of rotating closed-loop pulsating heat pipe from working fluid temperature. Appl Therm Eng. 2019; 148: 1303-9. https://doi.org/10.1016/j.applthermaleng.2018.11.030

[36] Qian N, Jiang F, Marengo M, Chen J, Fu Y, Zhang J, *et al*. Start-up behavior of oscillating heat pipe in grinding wheel under axial-rotation conditions. Appl Therm Eng. 2023; 219: 119443. https://doi.org/10.1016/j.applthermaleng.2022.119443

[37] Qian N, Fu Y, Zhang Y, Chen J, Xu J. Experimental investigation of thermal performance of the oscillating heat pipe for the grinding wheel. Int J Heat Mass Transf. 2019; 136: 911-23. https://doi.org/10.1016/j.ijheatmasstransfer.2019.03.065

[38] Czajkowski C, Nowak AI, Ochman A, Pietrowicz S. Flower shaped oscillating heat pipe at the thermosyphon condition: Performance at different rotational speeds, filling ratios, and heat supplies. Appl Therm Eng. 2022; 212: 118540. https://doi.org/10.1016/j.applthermaleng.2022.118540

[39] Czajkowski C, Nowak AI, Pietrowicz S. Flower shape oscillating heat pipe – A novel type of oscillating heat pipe in a rotary system of coordinates – An experimental investigation. Appl Therm Eng. 2022; 179: 115702. https://doi.org/10.1016/j.applthermaleng.2020.115702

[40] Qian N, Fu Y, Jiang F, Ding W, Zhang J, Xu J. CBN grain wear during eco-benign grinding of nickel-based superalloy with oscillating heat pipe abrasive wheel. Ceram Int. 2022; 48: 9692-701. https://doi.org/10.1016/j.ceramint.2021.12.170

[41] Qian N, Fu Y, Chen J, Khan AM, Xu J. Axial rotating heat-pipe grinding wheel for eco–benign machining: A novel method for dry profile-grinding of Ti–6Al–4V alloy. J Manuf Process. 2020; 56: 216–27. https://doi.org/10.1016/j.jmapro.2020.03.023

[42] Ebrahimi Dehshali M, Nazari MA, Shafii MB. Thermal performance of rotating closed-loop pulsating heat pipes: Experimental investigation and semi-empirical correlation. Int J Therm Sci. 2018; 123: 14-26. https://doi.org/10.1016/j.ijthermalsci.2017.09.009

[43] Czajkowski C, Błasiak P, Rak J, Pietrowicz S. The development and thermal analysis of a U-shaped pulsating tube operating in a rotating system of coordinates. Int J Therm Sci. 2018; 132: 645-62. https://doi.org/10.1016/j.ijthermalsci.2018.07.002

[44] Aboutalebi M, Nikravan Moghaddam AM, Mohammadi N, Shafii MB. Experimental investigation on performance of a rotating closed loop pulsating heat pipe. Int J Heat Mass Transf. 2013; 45: 137-45. https://doi.org/10.1016/j.icheatmasstransfer.2013.04.008

[45] Kammuang-lue N, Patanathabutr C, Sakulchangsatjatai P, Terdtoon P. Thermal characteristics of rotating closed-loop pulsating heat pipe designed for rotating-type energy storage devices. Energy Rep. 2022; 8: 302-8. https://doi.org/10.1016/j.egyr.2022.10.206

[46] Liou T-M, Chang SW, Cai WL, Lan I-A. Thermal fluid characteristics of pulsating heat pipe in radially rotating thin pad. Int J Heat Mass Transf. 2019; 131: 273-90. https://doi.org/10.1016/j.ijheatmasstransfer.2018.10.132

[47] Jang DS, Cho W, Ham SH, Kim Y. Thermal spreading characteristics of novel radial pulsating heat pipes with diverging nonuniform channels. Int J Heat Mass Transf. 2022; 199: 123488. https://doi.org/10.1016/j.ijheatmasstransfer.2022.123488

[48] Chen X, Liu X, Xu D, Chen Y. Thermal performance of a tandem-dual-channel flat-plate pulsating heat pipe applicable to hypergravity. Int J Heat Mass Transf. 2022; 189: 122656. https://doi.org/10.1016/j.ijheatmasstransfer.2022.122656

[49] Chen X, Chen S, Zhang Z, Sun D, Liu X. Heat transfer investigation of a flat-plate oscillating heat pipe with tandem dual channels under nonuniform heating. Int J Heat Mass Transf. 2021; 180: 121830. https://doi.org/10.1016/j.ijheatmasstransfer.2021.121830

[50] Qian N, Jiang F, Marengo M, Fu Y, Xu J. Thermal performance of a radial-rotating oscillating heat pipe and its application in grinding processes with enhanced heat transfer. Appl Therm Eng. 2023; 233: 121213. https://doi.org/10.1016/j.applthermaleng.2023.121213